Chemosphere 272 (2021) 129877

Contents lists available at ScienceDirect

Chemosphere

journal homepage: www.elsevier.com/locate/chemosphere

Evaluation of component additive modelling approach for europium adsorption on 2:1 clays: Experimental, thermodynamic databases, and models

Tiziana Missana*, Ursula Alonso, Miguel García-Gutiérrez

Centro de Investigaciones Energéticas Medioambientales y Tecnológicas (CIEMAT), Department of Environment, Avenida Complutense 40, 28040, Madrid, Spain

HIGHLIGHTS

- The component additive model predicts Eu adsorption on 2:1 clay mixture.
- Sorption modelling included: ion exchange and competition, and surface complexation.
- In the mixtures, smectite controls Eu adsorption when ion exchange predominates.
- Illite controls Eu retention when surface complexation predominates.
- Uncertainties related to modelling and to the use thermodynamic data are outlined.

GRAPHICAL ABSTRACT

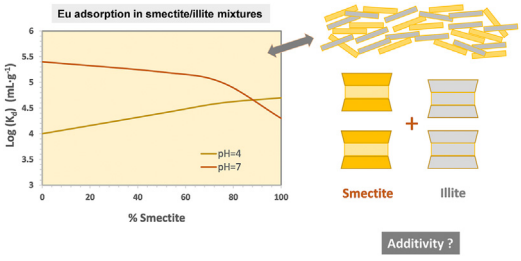

ARTICLE INFO

Article history:
Received 29 November 2020
Received in revised form
21 January 2021
Accepted 3 February 2021
Available online 9 February 2021

Handling Editor: Junfeng Niu

Keywords:
Adsorption
Clays
Europium
Component additivity approach
Ion competition
Thermodynamic databases

ABSTRACT

This study evaluates the component additive approach for Eu adsorption on mixtures of smectite and illite, which are the most common clays used as barriers for contaminant retention in waste repositories. A thorough set of Eu adsorption data for Na-exchanged smectite and illite that encompasses a wide range of pH values, ionic strengths, and Eu concentrations was provided. This database is likely one of the largest sorption databases available for Eu in 2:1 clays, making it appropriate for sorption model calibration.

The main adsorption mechanisms considered were surface complexation, on weak and strong clay edge sites, and cation exchange. Further, the role of principal ions, which are naturally leached from clays, as competitive factors for Eu retention, was evaluated in the modelling calculations. The main uncertainties related to the modelling procedures and the use of different thermodynamic data on sorption modelling were outlined.

The reactions and parameters successful in modelling Eu adsorption on individual clays were used without any modification to model Eu adsorption on illite/smectite mixtures, wherein only the relative mineral proportions were considered. The fit of the sorption data in the mixed clay system was satisfactory, indicating that, in 2:1 clays, Eu sorption is an additive process, which stresses the predictive capacity of the component additive approach in these systems. This is an important support for assessing the performance of barrier materials for contaminant migration under different geochemical conditions.

* Corresponding author.
E-mail address: tiziana.missana@ciemat.es (T. Missana).

https://doi.org/10.1016/j.chemosphere.2021.129877
0045-6535/

1. Introduction

Adsorption processes are fundamental for the elimination of undesired ions and molecules from aqueous phases and are thus relevant in areas related to pollution control, water treatment, and waste disposal.

Several different materials (clays, oxides, active carbon, zeolites, and various organic materials), natural or modified, have been analysed for the treatment of different types of contamination (Bonilla-Petriciolet et al., 2017). Clayey rocks are commonly employed as reactive barriers for pollutant containment, and smectite and illite are considered for use as engineered or natural barriers in high-level radioactive waste repositories (Norris, 2014; Sellin and Leupin, 2014). To assess the long-term safety of clayey barriers, it is necessary to further understand adsorption processes and develop mechanistic models that predict contaminant migration in the environment (Payne et al., 2013).

Natural materials are complex, heterogeneous, and their chemical conditions evolve with time. Thus, mechanistic studies of contaminant adsorption face several challenges and, consequently, their application to real systems remains limited. The mechanistic comprehension of complex systems is inevitably simplified, but it is important to ensure minimal loss of relevant information. The main methodologies proposed to model adsorption processes in complex/natural systems are the generalised composite (GCA) and component additivity (CAA) approaches (Davis et al., 1998). The GCA assumes that a complex material can be characterised in general terms without going in depth on its real nature. It is assumed that the material has "generic" surface sites, in which surface complexes are defined. The parameters necessary for modelling, including the specific surface area, cation exchange capacity (CEC), and surface acidity constants, are measured for the entire material in order to represent its mean properties. Even if the GCA can be useful as an operational tool to obtain general information on the adsorption properties of the system, it remains to be an empirical methodology.

Meanwhile, the CAA assumes that a natural material is formed by different minerals, each one with its own properties, and thus total adsorption depends on the contributions of each single component. This implies that the solid must be exhaustively characterised and the solid/contaminant interactions must be described in detail for each component, which favours a mechanistic understanding of the medium (Davis et al., 1998; Landry et al., 2009; Payne et al., 2013).

The main objective of this study was to analyse the application of the CAA for Eu adsorption in smectite and illite clay mixtures by providing a large experimental adsorption dataset that encompasses a wide range of pH values (from 3 to 11), ionic strengths (ISs, from 1×10^{-3} M to 2×10^{-1} M), and Eu concentration (from 5×10^{-10} M to 1×10^{-3} M), and focusing on the effects produced by the main ions leached from the clays, which cannot be completely eliminated in homoionisation and purification processes (Missana et al., 2014).

Further, this study aims to highlight the main uncertainties related to modelling work and the importance of the availability of robust thermodynamic databases for the application of mechanistic sorption models.

The selected element (^{152}Eu) is a lanthanide, which is often regarded as a chemical homologue of trivalent actinides, An^{3+} (Rabung et al., 2005), which has a rather complex aqueous chemistry. ^{152}Eu can be produced by neutron activation in nuclear reactor control rods, and is a fission product of U and Pu, making it of special interest for geochemical studies related to radioactive waste.

Previous studies on Eu retention in single 2:1 clay minerals that combine experimental investigation and modelling exist (Bradbury and Baeyens, 2002; Rabung et al., 2005; Bradbury et al., 2005; Tertre et al., 2005; Marques et al., 2008; Sasaki et al., 2016; Verma et al., 2019); Kumar et al. (2013) analysed adsorption on montmorillonite and kaolinite mixtures. However, there are no studies regarding the application of modelling to analyse Eu adsorption in 2:1 clay mixtures.

Contaminant retention on mixed solids is distinctive, and the CAA is not always successful, thus, adsorption additivity must not be taken for granted. The CAA has satisfactorily described Cs adsorption on mixed illite, smectite, and kaolinite (Cherif et al., 2017). Conversely, Alessi and Fein (2010) applied the CAA to analyse Cd adsorption in kaolinite mixed with oxy-hydroxides and, in some mixtures, the adsorption was underestimated. In smectite and alumina mixtures, the CAA adequately described selenite adsorption (Mayordomo et al., 2016), but underestimated Sr adsorption under acidic pH conditions, wherein cation exchanges dominate (Mayordomo et al., 2019). This effect was attributed to oxide/clay surface interactions and charge shielding, which hinder Sr retention. Hurel and Marmier (2010) analysed the CAA for Eu adsorption on the MX-80 bentonite and found that adsorption could only be predicted in a limited pH range (5.5–7.5); Bruggeman et al. (2010) used the CAA to interpret the influence of organic matter on Eu adsorption by illite. As different systems behave differently, detailed studies are necessary to guarantee the predictive capacity of adsorption models in complex environments.

To apply the CAA, it is necessary to develop independent models for each relevant component under the widest range of experimental conditions. Many studies on Eu adsorption in clays proposed models based on data obtained at a single IS or on adsorption edges at a single Eu concentration. Note that if the data are not complete enough, it is difficult to guarantee proper extrapolation to a different IS or contaminant concentration (Schnurr et al., 2015; Verma et al., 2019).

The materials selected for this study were a Spanish smectite (FEBEX bentonite, FBX) and French illite (Illite du Puy, IdP), which were previously exchanged in Na.

The ion exchange and competitive effects, surface complexation, and precipitation were evaluated to determine the Eu retention in both clays. A complete set of experimental data for Eu adsorption in the smectite and illite was required to outline the main processes involved in contaminant adsorption and to quantify their effects on the overall retention of the single components.

To check the validity of the CAA, the model parameters (selectivity coefficients and surface complexation constants) determined for the single clays were used to model the Eu sorption in the smectite/illite mixtures in two different proportions without any additional modification while accounting for the relative clay proportions.

2. Materials and methods

2.1. Adsorbents: smectite and illite clays

In this study, 2 previously well-characterised materials were used (FBX and IdP). The FBX is a Ca–Mg clay with a high smectite content (94% ± 3%). Its comprehensive characterisation is provided in the literature (Fernandez et al., 2004; Huertas et al., 2006). The IdP and has a high illite content (93%) with some and kaolinite (7%) (Gabis, 1958; Bradbury and Baeyens, 2005).

The clays, which were previously crushed and sieved (<64 μm), were converted to their Na-form by washing three times with 1 M $NaClO_4$. After the exchange procedure, the clays were distributed in centrifuge tubes and mixed with ultra-pure water. To obtain the fine clay fraction (<500 nm) and eliminate large mineral impurities,

the suspensions were centrifuged (600 g, 10 min) and the supernatant was collected in polyethylene bottles and flocculated with 1 M $NaClO_4$. The clay remaining in the centrifuge tubes was mixed with ultra-pure water and centrifuged again. The washing/centrifugation/supernatant collection cycle was repeated until enough solid material was available. There was no additional acid treatment to eliminate less soluble minerals (as carbonates) in order to prevent extensive clay dissolution.

The IS of the clay suspensions was changed via dialysis (Spectra Por Dialysis Membranes MWCO 3.5 kD) using $NaClO_4$ at different concentrations. The final clay concentration was determined via gravimetry, wherein 50 mL of the suspensions were dried in an oven for 2 days at 105 °C in triplicate. The clay concentration used in the sorption experiments ranged from 0.5 g L^{-1} to 1 g L^{-1}.

The total CECs of the Na-clays were measured using the copper triethylenetetramine (Cu-Trien or $[Cu(trien)]^{2+}$) method (Amman et al., 2005; Dohrmann and Kaufhold, 2009). The CECs were 100 ± 4 meq/100 g and 24 ± 2 meq/100 g for the Na-FBX and Na-IdP, respectively, which is consistent with previous studies (Fernandez et al., 2004; Rabung et al., 2005).

The external surface area was measured using the standard Brunauer-Emmet-Teller (N_2-BET) method with a Micromeritics ASAP 2020 V3.02H apparatus. The values were 59 ± 3 m^2 g^{-1} and 120 ± 4 m^2 g^{-1} for the Na-FBX and Na-IdP, respectively, which agrees with previous studies (Férnandez et al., 2004; Bradbury and Baeyens, 2005).

2.2. Adsorbate: europium

The isotope of europium used in this study was $^{152}Eu(III)$, which is from a carrier-free solution of $^{152}EuCl_3$, diluted in HCl, as supplied by Eckert and Ziegler isotope products. ^{152}Eu has a half-life of approximately 13.5 years, mainly decays by electron capture (72%), and is a hard gamma emitter. Its activity was measured via γ-counting with a NaI detector (Packard Auto-gamma COBRA 2).

2.3. Contact electrolyte

The electrolytes in equilibrium with the clay at different pH values (from 3 to 10) and ISs (from 1×10^{-3} M to 2×10^{-1} M) were analysed by filtering with a syringe filter of 0.2 μm (Millipore). Calcium and magnesium were analysed using inductively coupled plasma atomic emission spectrometry (ICP-AES Varian 735 ES). Sodium and potassium were determined using atomic absorption spectrometry (Varian AA240 FS), and the carbonates were determined by potentiometric titration (Metrohm 888 Titroprocessor).

2.4. Sorption experiments

Batch sorption experiments were conducted in a glove box under a N_2 atmosphere at room temperature (23 ± 2 °C). Na-FBX, Na-IdP, and their suspensions at different ISs were used for the experiments. The adsorption of the illite-smectite mixtures was analysed, mixing the smectite and illite suspension at an IS of 5×10^{-2} M at two different Na-FBX/Na-IdP ratios (50%/50% and 75%/25%) with a total clay concentration of 0.5 g L^{-1}.

The kinetics of the sorption process were analysed first to determine the appropriate experiment time for further sorption experiments.

Europium sorption as a function of pH was analysed by performing "sorption edges" at pH values of 3–11 at different ISs and an Eu concentration of $6.9 \times 10^{-9} - 9.9 \times 10^{-9}$ M. The pH was changed by adding NaOH/HCl 0.1 M, and buffer solutions were used to maintain a stable pH over time. The buffer solutions used for each pH range are summarised in the Supporting Information (Table 1S). Note that they were used at a concentration of 2×10^{-3} M, which has been proven to not affect Eu retention.

Sorption isotherms were obtained at a fixed pH and background electrolyte concentration by varying the Eu concentration (from 5×10^{-10} to 9×10^{-4} M). Concentrations higher than 1×10^{-7} M were achieved by adding stable Eu, which was derived from $EuCl_3$ high purity salts, to the radioactive ^{152}Eu.

Ultracentrifuge polypropylene tubes (12.5 mL) were filled with the samples for the sorption study. Then, they were sealed with heat and underwent continuous stirring until phase separation. The solid/liquid separation was carried out by ultra-centrifugation (645,000 g, 30 min) with a Beckman L90-Ultra ultracentrifuge. The effectiveness of the solid/liquid separation was validated by determining the concentration of colloids using photon correlation spectrometry with a Malvern 4700 apparatus with a 4 W Ar laser (514 nm), as described in the literature (Missana et al., 2008).

Three aliquots of the supernatant were taken from each tube to measure the final Eu concentration in the supernatant (Eu_{LIQ}). The rest of the solution was used to measure the final pH. The relationship between the adsorbed Eu concentration (Eu_{ADS}) and that remaining in the liquid (Eu_{LIQ}) is defined as the distribution coefficient (Kd):

$$K_d = \frac{[Eu_{ADS}]}{[Eu_{LIQ}]} = \frac{Eu_{INI} - Eu_{LIQ}}{Eu_{LIQ}} \cdot \frac{V}{m}, \qquad \text{Equation 1}$$

where Eu_{INI} is the initial Eu concentration, m is the mass of the clay (g), and V (mL) is the volume of the electrolyte. K_d is expressed in mL·g^{-1} units. Depending on the pH and IS, the K_d values for Eu can span several orders of magnitude. Therefore, the sorption data were expressed as log (K_d). The representation of data as a percentage of adsorption $\left(100 \cdot \frac{Eu_{ADS}}{Eu_{INI}}\right)$ was discarded because it is not sensitive enough to reveal data variation, and subsequently perform sorption modelling, especially when sorption is high (Payne et al., 2013).

The largest experimental error in the sorption tests was observed in the region of the highest Eu adsorption (high pH and/or low IS), whereas the maximum log (K_d) error was estimated to be less than 5% under all experimental conditions. Thus, an uncertainty of 5% in the log (K_d) data fully covers the experimental error and has been indicated in all the experimental points.

Eu sorption on the ultracentrifuge tubes was checked after the sorption tests. As it was found to be lower than 2%, it was not accounted for in the K_d calculations.

2.5. Modelling of adsorption data

Smectite and illite are layered aluminosilicates formed by two tetrahedral (T) and one octahedral (O) layers that are ordered in a TOT structure (2:1 clays) (Odom, 1984). They possess a negative permanent charge caused by isomorphic substitutions in their structure, which is compensated by the presence of cations in their interlayers (Bergaya and Lagaly, 2013). In addition to this constant charge, corresponding to the CEC, the clay surface has a smaller variable charge from the amphoteric functional groups at the particle edges, which is where the Si–O–Si and Al–O–Al bonds are broken (silanol and aluminol groups, respectively).

These permanent and pH-dependent charge contributions lead to different sorption mechanisms for the cations, such as cation exchange and surface complexation. Regarding Eu, different spectroscopic studies have confirmed the formation of outer-sphere complexes under acidic pH conditions (where cationic exchanges prevail), and inner-sphere complexes at neutral to basic pH conditions (Stumpf et al., 2004; Kowal-Fouchard et al., 2004a; Sheng

et al., 2009; Sasaki et al., 2016; Huittinen et al., 2010; Marques et al., 2016). Nevertheless, there is no general agreement between the number or type of surface sites or complexes proposed.

2.5.1. Cation exchange

In an Na-exchanged clay, Na is the (unique) cation that balances the surface negative charge and can be substituted by another cation present in solution (e.g., cation B, with valence z_B). As Na ≡ X represents the exchange site at the Na-clay surface, the exchange reaction can be expressed as:

$$z_B(Na \equiv X) + B \leftrightarrow (B \equiv X) + z_B Na. \quad \text{Equation 2}$$

If cation B is present at trace levels and the Na–B exchange is the predominant sorption mechanism, according to the Gaines and Thomas (1953) theory, the selectivity coefficient can be obtained using the measured K_d value as follows (Bradbury and Baeyens, 2002):

$${}^{B}_{Na}K_{SEL} = \left[\frac{K_d \cdot z_B}{CEC}\right] \frac{(\gamma_{Na})^{z_B}}{\gamma_B}(Na)^{z_B}, \quad \text{Equation 3a}$$

where γ_{NA} and γ_B are the solution activity coefficients of Na and the cation B, respectively, and CEC is the cation exchange capacity of the clay. In the case of Eu–Na exchange ($z_B = 3$), the selectivity coefficient is determined using the following:

$${}^{Eu}_{Na}K_{SEL} = \left[\frac{K_d \cdot 3}{CEC}\right] \frac{(\gamma_{Na})^{3}}{\gamma_{Eu}}(Na)^{3}, \quad \text{Equation 3b}$$

In an ionic exchange process, the IS is expected to play an important role in retention because the log (K_d) of cation B in electrolyte A depends, theoretically, on the electrolyte concentration according to the following:

$$z_A \cdot Log(K_d) = -z_B \cdot Log(A) + Log\left(\frac{{}^{B}_{A}K_{SEL} \cdot (CEC)^{z_A} \cdot \gamma_B^{z_A}}{z_B^{z_A} \cdot \gamma_A^{z_B}}\right). \quad \text{Equation 4}$$

Thus, in the absence of any other competing ion, log (K_d) depends linearly on the logarithm of the concentration of A (log (A)), wherein the slope of this straight line is $-z_B/z_A$. In the case of Eu–Na exchange, the z_B/z_A value is 3. Thus, the exchange process was evaluated not only for Eu but also for other possibly competitive cations present in solution (K, Ca, Mg, and Al).

2.5.2. Surface complexation

Surface complexation reactions occur at the amphoteric functional groups (SOH) present on the clay surface. The pH-dependent charge at the clay surface is determined by the protonation/deprotonation reactions at these sites, which is similar to what occurs in oxides:

$$SOH_2^+ \Leftrightarrow SOH + H^+, \quad \text{Equation 5a}$$

$$SOH \Leftrightarrow SO^- + H^+, \quad \text{Equation 5b}$$

where SOH_2^+, SOH, and SO^- represent the positively charged, neutral, and negatively charged surface sites, respectively.

The adsorption of cations on these SOH groups can be described as expressed in Equation (6), in which M^{z+} is a generic cationic species in solution:

$$SOH + M^{z+} \Leftrightarrow SOM^{z-1} + H^+. \quad \text{Equation 6}$$

To interpret the surface complexation, one must first select a model, in which the choice is somewhat subjective; the general tendency is to use "simple" models, but different approximations can fit the experimental data.

Previous attempts to theoretically describe Eu adsorption on individual clays have been made, wherein the fitting approaches varied. Bradbury and Baeyens (2002) and Marques et al. (2008) used a quasi-mechanistic 2-site protolysis non-electrostatic surface complexation and cation exchange model (2SPNE/CE). Apart from the exchange sites, the 2SPNE/CE assumes the existence of one strong and two weak sites at the clay surface. However, for contaminant complexation, they used only the strong site, or the strong site and one weak site. Sasaki et al. (2016) selected a 1-site non-electrostatic model (NEM); Tertre et al. (2006) and Guo et al. (2009) used electrostatic (diffuse double layer) models, which assumed the existence of different sites on clay (one or two aluminols, and one silanol), but their Eu modelling only considered the complexation on aluminols. Other electrostatic models, such as the constant capacitance and triple layer model, have been applied to explain complexation reactions on clays (Kowal-Fouchard et al., 2004b; Goldberg, 2014).

In this study, to model the surface complexation reactions, a standard 2-site (weak, S_wOH, and strong, S_sOH) NEM was selected because it has been satisfactorily used to fit the sorption data of other elements in Na-FBX and Na-IdP (Missana et al., 2009a, 2009b). Further, note that, at a mechanistic level, the contribution of two sites with different densities and selectivities can be related to the existence of aluminol and silanol clay sites.

2.6. Model calculations and thermodynamic databases

The calculations of Eu aqueous speciation and adsorption were conducted using the Chess v2.4 code (Van der Lee and de Windt, 1999), and the B-dot equation was used as an activity model.

The fit of the sorption data was determined by conducting a trial-and-error procedure, changing the fitting parameters (selectivity coefficients and surface complexation constants) in the input, and comparing the calculated values with the experimental results.

The selection of a thermodynamic database (TDB) is crucial because TDBs are indispensable tools for computing the contaminant aqueous speciation, and channel the consequent selection of the complexing species contributing to sorption. To date, a general agreement on the ideal TDB for calculating Eu speciation does not exist, and updated Eu data are scarce. The Nuclear Energy Agency of the Organisation for Economic Co-operation and Development (OECD-NEA) provides periodic updates of thermodynamic data for most radioactive elements, but not for Eu. For this reason, some authors use (part of) the database published by the OECD-NEA for Am^{3+} (Guillamont et al., 2003).

In this study, for modelling purposes, two databases were used (EQ (3)/6 and ThermoChimie). EQ (3)/6 database (Delany and Lundeen, 1991), compiled by the Lawrence Livermore National Laboratory, is the database originally provided with the Chess code, while the ThermoChimie (Grivé et al., 2015) is a database compiled by the French National Radioactive Waste Management Agency (Andra), and is mainly based on OECD-NEA books, when available. Most of the constants selected by the ThermoChimie database for Eu-hydrolysed and carbonate species were taken from Spahiu and Bruno (1995) and references therein.

The objective of using two databases is to not discuss or judge the species and constants of each, but rather to highlight the consequences of different choices on sorption modelling. The main species used for the calculations and their stability constants, as provided by each TBD, are listed in Tables 2S and 3S The principal outcomes and differences are examined in Section 3.

3. Results and discussion

3.1. Contact electrolyte analysis

Among the ions found in the solutions in contact with clay, those that were examined as potentially competitive ions for Eu sorption at the clay exchange sites included monovalent potassium, divalent ions (calcium and magnesium), and trivalent aluminium. The concentrations of these ions were measured in the supernatants of the clay suspensions used for the sorption tests under different pH and IS conditions (Table 4S). For Na-FBX, the results were: $[K^+] = 1.4 \times 10^{-5} - 5.2 \times 10^{-5}$ M, $[Ca^{2+}] = 9.5 \times 10^{-6} - 4.3 \times 10^{-4}$ M, and $[Al^{3+}] < 2 \times 10^{-6}$ M. For Na-IdP, the results were: $[K^+] = 1.2 \times 10^{-5} - 1.5 \times 10^{-4}$ M, $[Ca^{2+}] = 5.0 \times 10^{-6} - 1.0 \times 10^{-4}$ M, and $[Al^{3+}] < 5 \times 10^{-5}$ M.

The ion present at higher concentrations was calcium, and the concentration of aluminium was always below 2×10^{-6} M in the Na-FBX, whereas in the Na-IdP it reached values of up to one order of magnitude higher. The mean quantities of HCO_3^-, which were measured at a pH of 7 in the aqueous solution in contact with the clay, were $1.1 \times 10^{-3} \pm 0.1 \times 10^{-3}$ M and $1.4 \times 10^{-3} \pm 0.0 \times 10^{-3}$ M for the Na-FBX and Na-IdP, respectively. The carbonates naturally present in clays are important for Eu speciation and must also be accounted for in the modelling.

3.2. Europium speciation

Europium speciation was calculated as a function of pH, wherein [Eu] = 1 × 10 M in $NaClO_4$ 0.1 M, with the constants listed in Tables 2S (EQ3/6) and 3 S (ThermoChimie), and the precipitation of solid species (in grey in Tables 2S and 3S) was initially allowed.

The resulting speciation using EQ (3)/6 database is shown in Fig. 1(a) and (b), wherein the latter focuses on the species present at lower concentrations. According to this database, the main species present at a pH less than 6.5 is trivalent cation Eu^{3+}. Meanwhile, under neutral and alkaline pH values, the main species predicted are $EuOHCO_3(aq)$, $EuCO_3^+$, $Eu(OH)_2CO_3^-$, and $EuOH(CO_3)_2^{2-}$. All the main species present at a pH higher than 7 are neutral or negatively charged. Thus, they are not expected to contribute to Eu retention. The "zoom" in Fig. 1b shows another positively charged species existing in the alkaline region: namely $Eu(OH)_2^+$.

For a comparative analysis, the Eu speciation using the ThermoChimie database was calculated under the same conditions previously adopted, and the results are shown in Fig. 1S (Supporting Information).

The first observed difference is related to the solubility of the solid species. While no precipitation was predicted by EQ (3)/6 database for [Eu] = 1×10^{-8} M, according to the ThermoChimie database (Fig. 1S), extensive Eu precipitation above a pH of 7 was predicted, wherein the main precipitated solids would be $Eu(CO_3)OH(cr)$ and $Eu(OH)_3$ (cr). However, such extensive Eu precipitation, which is usually observable in the shape of the sorption isotherms, was not experimentally observed. The solubility of Eu in the presence of carbonates may vary depending on the formation of mixed hydrolysed, crystalline, or aged-with-time solid phases (Runde et al., 1992; Fanghänel and Neck, 2000).

To obtain more information on the aqueous species, the calculation was repeated, excluding solid precipitation (Fig. 2S(a-b) in Supporting Information). The main differences in the speciation calculated with the two TDBs depended on the consideration of certain mixed hydroxo-carbonate species, such as $EuOH(CO_3)$ (aq). The stoichiometries considered for the formation of Eu^{3+} complexes with (bi)carbonates were different in each database. While some studies (Rao and Chatt, 1988) found that both $Eu(HCO_3)_i^{3-i}$ and $Eu(CO_3)_i^{3-2i}$ stoichiometries can co-exist, others only considered the existence of $Eu(CO_3)_i^{3-2i}$, which is consistent with trivalent actinides, such as Am. Even though these mixed hydroxo-carbonate species were omitted, their existence was not completely discarded (Plancque et al., 2003; Vercouter et al., 2005), thereby providing the principal source of uncertainty. Further, the exclusion of $EuOH(CO_3)(aq)$ in the ThermoChimie TDB makes that $EuCO_3^+$ predominates in the speciation diagram at much higher concentrations and at a wider range of pH than that of EQ (3)/6 TDB, even if the formation constant for $EuCO_3^+$ is very similar in each (Tables 2S and 3S).

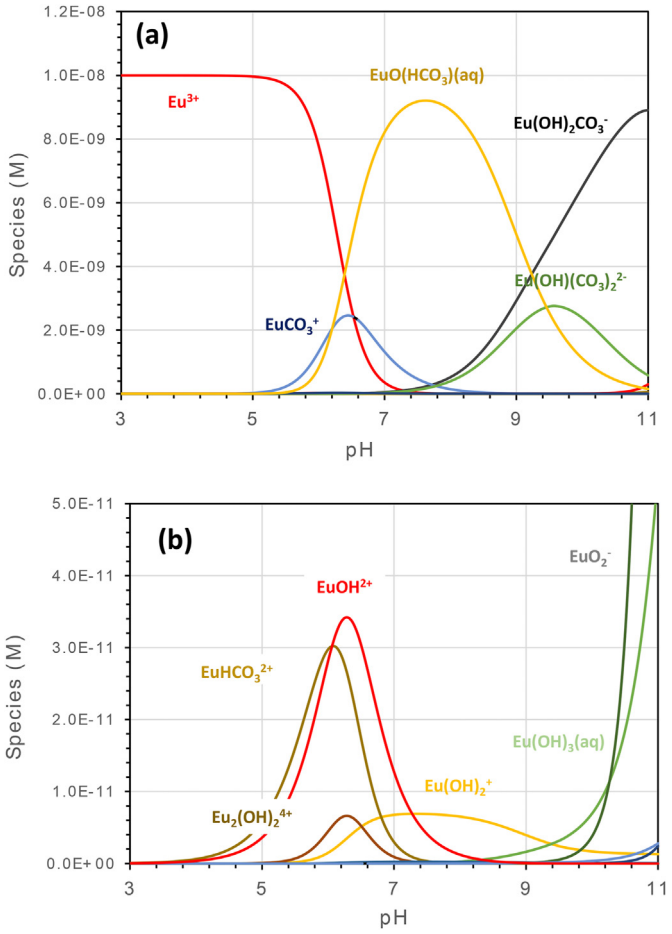

Fig. 1. Europium speciation in $NaClO_4$ 0.1 M [Eu] = 1×10^{-8} M. Main species present in concentration (a) higher than 1×10^{-10} M, and (b) lower than 1×10^{-10} M. Calculations were performed with EQ (3)/6 database. Precipitation allowed.

3.3. Sorption tests on single minerals

3.3.1. Kinetic

Preliminary kinetic tests (from 1 h to 30 d) were carried out for Na-FBX and Na-IdP at 0.1 M $NaClO_4$ and different pH values. The results of these tests are shown in the Supporting Information (Fig. 3S). In both clays and at all the pH values investigated, Eu uptake was very rapid (<1 d). For all experiments, the contact time was fixed to 7 d.

3.3.2. Sorption edges

Fig. 2 shows the Eu adsorption edges at different ionic strengths, Fig. 2a shows the results obtained with Na-FBX ([Eu] = 9.9×10^{-9} M) and Fig. 2b shows the results obtained

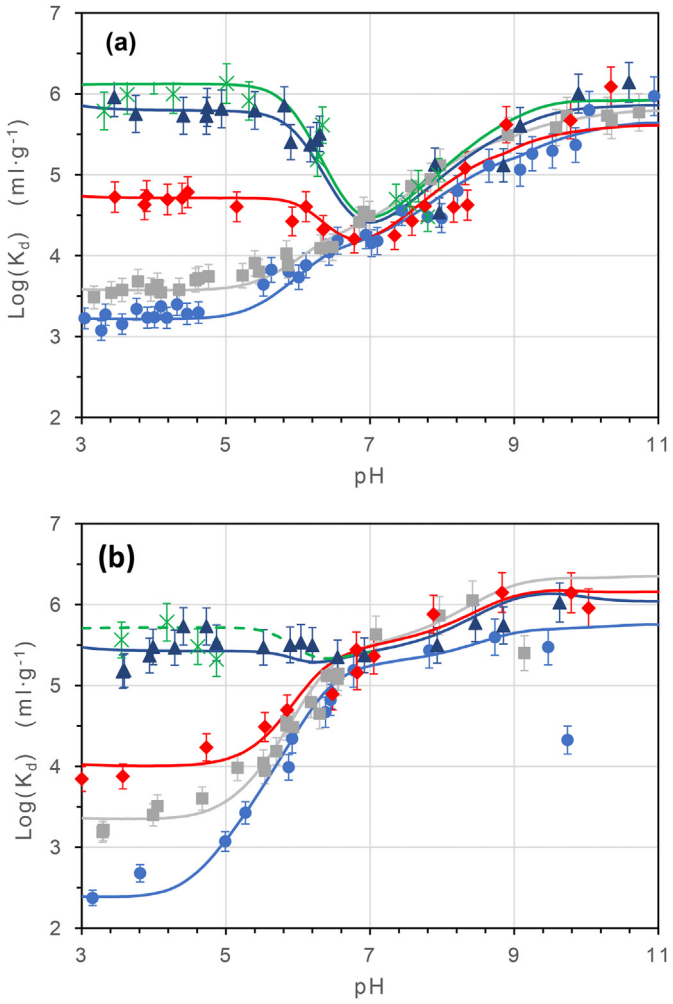

Fig. 2. Sorption edges for Eu in (a) Na-Illite du Puy (IdP) and (b) Na- FEBEX bentonite (FBX) at different ionic strengths in $NaClO_4$. (●) 0.2 M, (■) 0.1 M, (◆) 0.05 M, (▲) 0.01 M, and (∗) 0.001 M. Lines correspond to the model calculations with parameters summarised in Table 1. Sorption data expressed as the logarithm of the distribution coefficient (K_d).

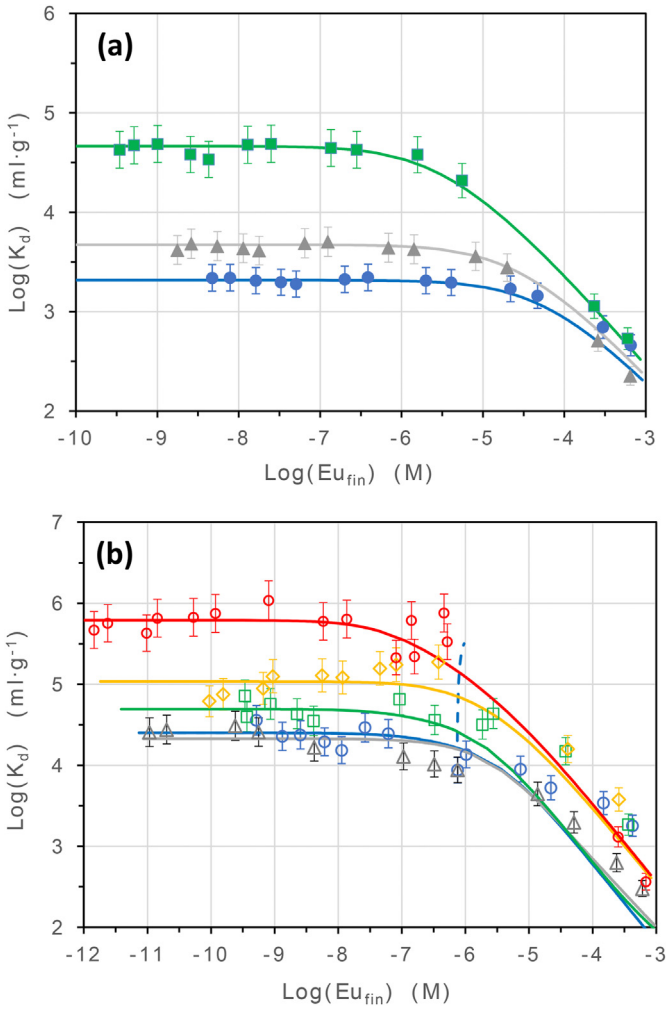

Fig. 3. Sorption isotherms of Eu in Na-FEBEX bentonite (FBX) in NaClO4 at different ionic strengths. (a) pH < 5: (●) I = 0.2 M and pH = 4.1; (▲) I = 0.1 M and pH = 3.8; and (■) I = 0.05 M and pH = 3.9. (b) pH > 5: (○) I = 0.001 M and pH = 6.0; (◇) I = 0.01 M and pH = 6.3; (□) I = 0.05 M and pH = 7.7; (△) I = 0.1 M and pH = 6.7; and (○) I = 0.2 M and pH = 7.4. Lines correspond to model calculations with the parameters summarised in Table 1 (EQ (3)/6 thermodynamic database). Dashed vertical line indicates the concentration where precipitation is predicted at a pH of 7.4.

with Na-IdP ([Eu] = 6.9×10^{-9} M). In these figures, three zones can be distinguished. In the first zone, which occurs at a more acidic pH (3–5), making the main aqueous species is Eu^{3+}, sorption significantly depends on the IS and exhibits only minimal variation with the pH, especially in the case of Na-FBX. In this region, the measured log (K_d) varied significantly from the highest to lowest IS from approximately 3 to 6 in the Na-FBX, and from 2.5 to 5.5 in the Na-IdP. Thus, adsorption may be related to the Eu^{3+}-Na^+ cationic exchange process, which is expected to be independent of the pH but dependent on the electrolyte concentration (Equation (4)).

In the second zone (pH values of 5–7), adsorption began to vary with pH, and the log (Kd) values either increased or decreased depending on the IS of the suspensions. In this pH region, the main charged species were Eu^{3+} and $EuCO_3^+$.

In this zone, the effect of the Eu^{3+}-Na^+ cationic exchange was still observable, but the positively charged species began contributing to Eu retention via surface complexation. At a pH greater than 7, the adsorption behaviour was similar at all ISs, varied with pH, suggesting that inner-sphere surface complexation was the main adsorption mechanism in this zone. Despite the presence of the aqueous bicarbonate leached by the clays in the system, the drastic decrease in sorption at a pH of 8 that has been observed by other researchers working under atmospheric pCO_2 conditions (Marques et al., 2008; Guo et al., 2009), was not observed herein.

Herein, at a high pH, large data scattering exists. This is somewhat expected because of the remarkably high Eu retention, but other factors may be involved, such as Eu incipient precipitation, which is highly dependent on pH (Fanghänel and Neck, 2000), or the presence of clay colloids. Na-clays, especially Na-smectites, can produce a large quantity of colloids, especially at low ISs (Missana et al, 2018b, 2018a). The presence of colloids in the supernatant was checked using photon correlation spectrometry to evaluate their potential impact on the K_d. The results showed that the particle concentration was always lower than 1–2 mg L^{-1}, reaching 7.5 mg L^{-1} in only in a few samples. These rare high values are probably related to an accidental resuspension of the clay during sampling, not to insufficient centrifugation. The possible impacts on K_d determination are shown in Fig. 3S, which includes the measured log (K_d) versus the real log (K_d) both in the absence of colloids and in the presence of different particle concentrations. When sorption is very high (log (K_d) > 5.5), the presence of colloids

causes a decrease in the measured log (K_d), which could exceed the estimated 5% error, and may cause the data dispersion.

3.3.3. Sorption isotherms

Figs. 3 and 4 show the adsorption isotherms obtained for Na-FBX and Na-IdP at different IS and pH values. Figs. 3(a) and 4(a), illustrate the isotherms obtained at pH values of less than 5 and Figs. 3(b) and 4(b) show the isotherms obtained at pH values greater than 5. The data are expressed as log (K_d) versus log (Eu_{fin}), instead of the previously used log (Eu_{ads}) versus log (Eu_{fin}) form to better delineate differences in the curves.

The shapes of the isotherms were similar for both clays. Sorption as a function of the Eu concentration revealed a zone in which K_d is approximately constant (linear sorption), and a zone in which the log (K_d) decreases with increasing Eu concentration, which is the result of the progressive saturation of sorption sites, followed by a Langmuir-type behaviour, which does not indicate extensive Eu precipitation.

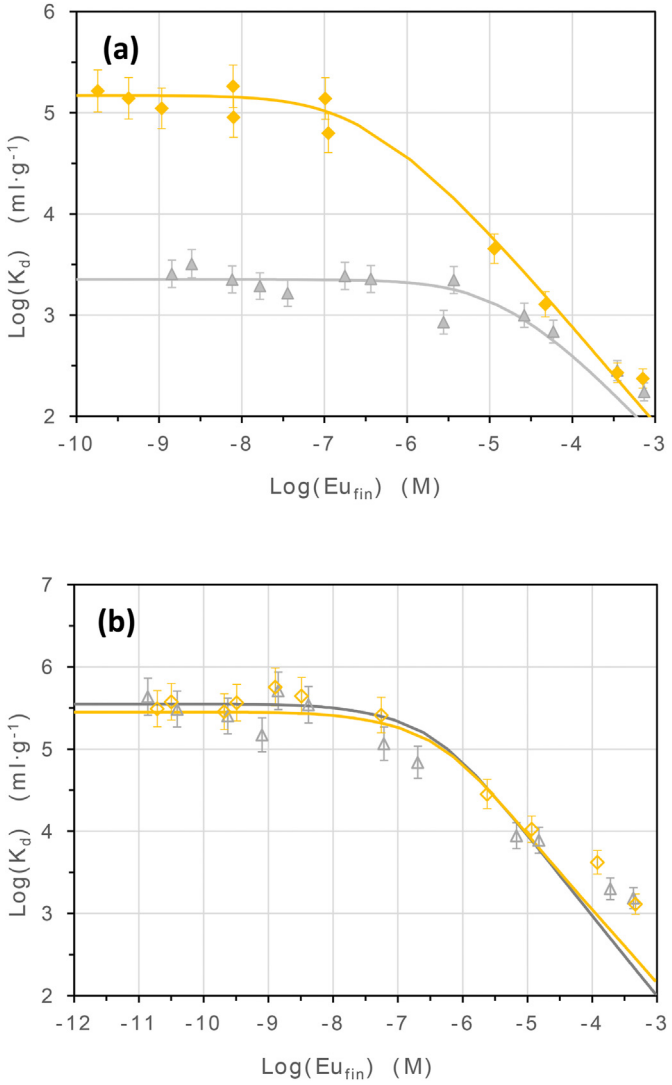

Fig. 4. Sorption isotherms of Eu in Na-Illite du Puy (IdP) in NaClO4 at two different ionic strengths. (a) pH < 5: (◆) I = 0.01 M and pH = 3.9; and (▲) I = 0.1 M and pH = 4.0; (b) pH > 5: (◇) I = 0.01 M and pH = 7.2; and (△) I = 0.1 M and pH = 7.2. Lines correspond to model calculations with the parameters summarised in Table 1 (EQ (3)/6 thermodynamic database).

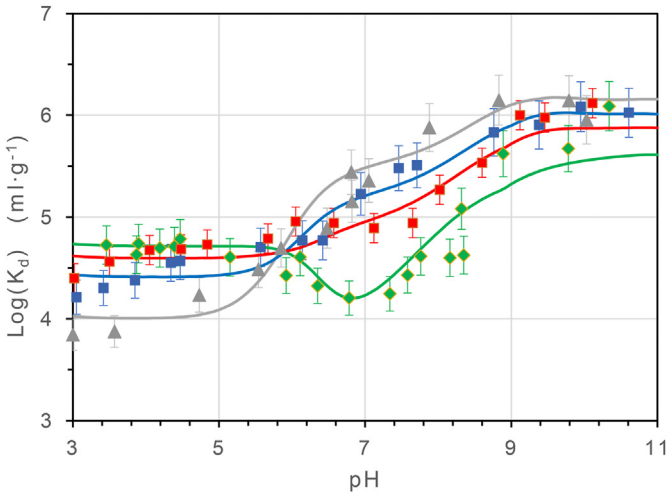

Fig. 5. Sorption edges of Eu in Na-FEBEX bentonite (FBX) and Na-Illite du Puy (IdP) in different proportions at the ionic strength of 0.05 M in NaClO4. (◆) 100% Na-FBX; (■) 50% Na-FBX and 50% Na-IdP; (■) 75% Na-FBX and 25% Na-IdP; and (▲)100% Na-IdP. Lines correspond to model calculations with the parameters summarised in Table 1 (EQ (3)/6 thermodynamic database). Sorption data expressed as the logarithm of the distribution coefficient (K_d).

3.4. Sorption tests on Na-FBX and Na-IdP mixture

Fig. 5 shows the sorption edges obtained for the two Na-FBX and Na-IdP mixtures (50% Na-FBX/50% Na-IdP and 75% Na-FBX/25% Na-IdP) in $NaClO_4$ at an IS of 5×10^{-2} M. The results obtained for 100% Na-FBX and 100% Na-IdP (5×10^{-2} M) were also included for comparison.

The curves intersect at a pH of approximately 6. In the region below this pH, sorption was higher when the smectite content was higher and cationic exchange predominated. Conversely, above a pH of 6, the sorption behaviour was inverted, wherein sorption increased with increasing illite content, indicating that the illite surface complexation sites are more selective than those of smectite.

3.5. Sorption modelling: individual clay components

3.5.1. Cation exchange and ion competition

The acidic pH region, wherein sorption clearly depends on IS, not pH (Fig. 2), is related to sorption by cation exchange. In this region, the main solute species is Eu^{3+}, which is the unique species that contributes to sorption.

The cation exchange reaction can be expressed as:

$$3 \cdot (Na \equiv X) + Eu^{3+} \leftrightarrow (Eu \equiv X) + 3Na. \qquad \text{Equation 7}$$

The dependence of the cationic exchange process on IS was evaluated and compared with the theoretical behaviour (Fig. 6). Each sorption test performed at pH values less than 4, was used to estimate the (apparent) selectivity coefficients (K_{SEL}) using Equation (3b). The log (K_{SEL}) and log (K_d) values were plotted as a function of the logarithm of the Na concentration (Fig. 6a and b, respectively).

At higher ISs, the calculated selectivity coefficients (marked within a box) were similar, but when the IS fell below 5×10^{-2} M, they significantly decreased (Fig. 6a). Equation (4) indicates that the theoretical relationship between log (K_d) and log (Na) for a binary Eu−Na exchange should be linear with a slope of −3 (dotted curves in Fig. 6b). Such a linear relationship was not experimentally observed, suggesting that the theoretical curves at low to

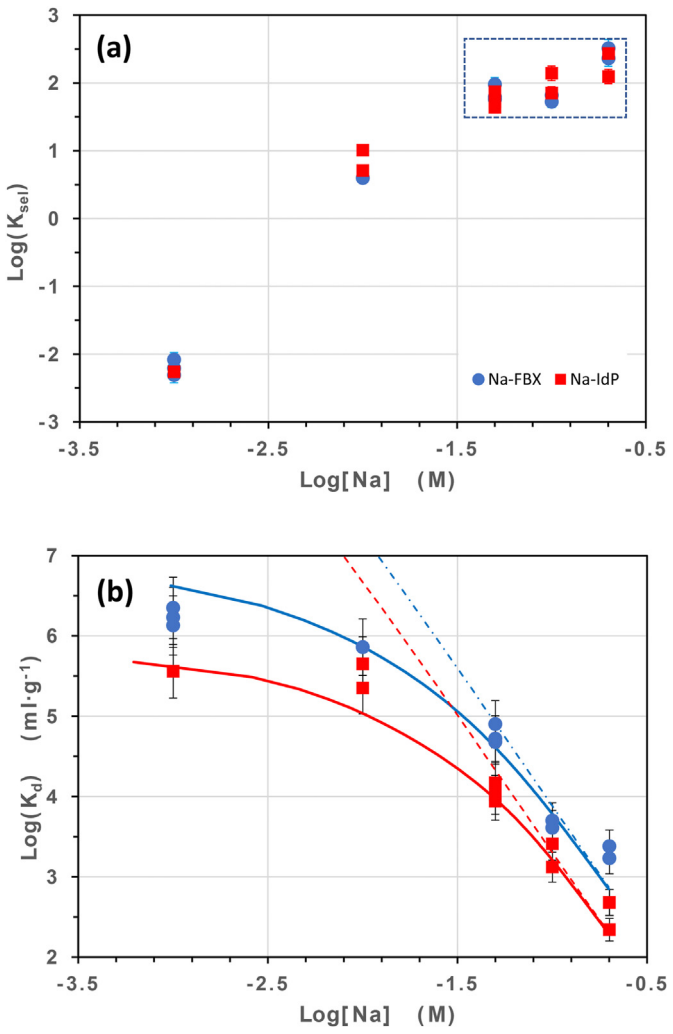

Fig. 6. Eu sorption as a function of ionic strength. a) Logarithm of the apparent selectivity coefficients (logKsel) as a function of ionic strength. The box indicates the values at higher ionic strengths. b) Dependence of log (K_d) on ionic strength. The dotted lines indicate the theoretical behaviour, and the continuous lines represent calculations considering the presence of competing cations.

intermediate ISs had highly overestimated sorption rates.

This is a clear indication that strong competitive effects exist, and that competitive ions must be accounted for, because their presence can bias the determination of selectivity coefficients (Missana et al., 2014). Thus, the effects of K^+, Ca^{2+}+Mg^{2+}, and Al^{3+} within the experiment concentration range were analysed in both clays using the selectivity constants listed in the literature for Na-FBX and Na-IdP, as summarised in Table 4S. The calculations revealed that potassium does not affect Eu retention in the clays; in Na-FBX, the aluminium concentration was lower than 1×10^{-6} M, suggesting it did not affect Eu sorption in smectite. Conversely, in Na-IdP, trivalent aluminium was present at a high enough concentration to influence Eu retention. Further, the presence of divalent ions, especially Ca, was non-negligible in both clays. Therefore, the calcium in both clays and aluminium in the Na-IdP were included in the calculation to evaluate the competitive effects.

As shown in Fig. 6b, the results fit reasonably well the experimental points at all ISs. The fit was obtained using the logarithm of the selectivity coefficient, $log(^{Eu}_{Na}K_{SEL})$, which were 2.00 and 2.03 for Na-FBX and Na-IdP, respectively, a fixed pH of 3.75, and included the competitive effects of Ca^{2+} (3.1×10^{-4} M) in the Na-FBX, and Ca^{2+} and Al^{3+} in the Na-IdP (6×10^{-5} M and 2×10^{-5} M, respectively). Therefore, the selectivity coefficient was constant in a wide range of ISs (1×10^{-3} to 2×10^{-1} M), assuming that the competitive ions were adequately accounted for in the model. The estimation of error was approximately ±0.3. Further, the selectivity coefficients estimated for both Na-FBX and Na-IdP were remarkably similar.

3.5.2. Surface complexation

To model Eu adsorption at pH values of greater than 5, it is necessary to consider the contribution of surface complexation. The 2-site NEM proposed in this study includes two types of sorption sites (S_wOH, weak, and S_SOH, strong). The densities of the weak/strong sorption sites and their protonation constants for both clays were 6.01×10^{-5}/2.01×10^{-6} eq·g^{-1} for Na-FBX, and 9.03×10^{-5}/$2.00 \cdot 10^{-6}$ eq·g^{-1} for Na-IdP, as determined in a previous work (Missana et al., 2008). The protonation constants of the sites are listed in Table 1.

Based on the speciation diagrams (Figs. 1, 2S and 3S), species were selected according to their concentration, range of pH in which they appear, and their charge. Above a zero charge (pH_{PZC}) of the solid (Equations 5a-b), the overall surface charge is negative. Therefore, positively charged species are expected to interact with the clay surface and be adsorbed (Equation (6)). Based on these criteria, in both EQ (3)/6 and ThermoChimie TDBs, the tested species were Eu^{3+}, $EuCO_3^+$, and $Eu(OH)_2^+$, which likely form monodentate inner-sphere surface complexes with both weak and strong sites, in accordance with the following reactions:

$$(1)\ SOH + Eu^{3+} = SO - Eu^{2+} + H^+, \qquad \text{Equation 8a}$$

$$(2)\ SOH + EuCO_3^+ = SO - EuCO_3 + H^+, \qquad \text{Equation 8b}$$

$$(3)\ SOH + Eu(OH)_2^+ = SO - Eu(OH)_2 + H^+. \qquad \text{Equation 8c}$$

After the selection of complexing species and their respective reactions, sorption edges simulations were performed to evaluate each species contribution to sorption at different pH regions. The sorption edges illustrated in Fig. 2 were conducted at relatively low Eu concentrations of $6.8 \times 10^{-9} - 9.8 \times 10^{-9}$ M, which fall within the linear zone of the sorption isotherms (Figs. 3 and 4). At this Eu concentration, strong sites are expected to control sorption, however, to properly fit the sorption behaviour at all the Eu concentrations, it is necessary to adjust the contribution of strong and weak sites. This is done by iteratively checking the simulations of the sorption edges and isotherms in a determinate pH zone, and simultaneously search for the best fit of both datasets at once.

Note that the Eu^{3+} species is the most important species present under both acidic and neutral pH conditions. In addition, under these conditions, Na^+-Eu^{3+} exchange is the dominant process if the IS is medium to low (<5×10^{-2} M), especially in the case of Na-FBX.

This means that, in this region, the contribution of other inner-sphere surface complexes could be determined only at high ISs, where cation exchange is lower; at lower ISs, their presence might be masked and not well isolated. This highlights the importance of evaluating sorption over a wide range of ISs.

Finally, even if simulations are diligently conducted, the solution to the chemical problem might not be unique because of the unavoidable degree of subjectivity in the simplification application choice, as well as the model, database, and complex selection. Despite disparities in databases, the selection of complexes must be thorough, and their reliability must be verified for a large amount of data and conditions. During the fitting processes, many possibilities are ruled out because they do not meet the experimentally observed dependences for IS, pH, or Eu concentration, as they are

Table 1
Surface complexation reactions used to model experimental data (in addition to ion exchange).

EQ (3)/6				
Surface Species		Composition	Na-Illite du Puy (IdP)	Na- FEBEX bentonite (FBX)
			log K	log K
S_1	**$S_wO\text{-}Eu^{2+}$**	1 S_sOH, 1 Eu^{3+}, −1 H^+	**0.6 ± 0.0**	**−0.05 ± 0.0**
S_2	**$S_wO\text{-}EuCO_3$**	1 S_sOH, 1 Eu^{3+}, 1 HCO_3^-,-2 H^+,	**−2.10 ± 0.14**	**−3.36 ± 0.18**
S_3	**$S_wO\text{-}Eu(OH)_2$**	1 S_sOH, 1 Eu^{3+}, −3 H^+, 2H_2O	**−13.75 ± 0.25**	**−13.62 ± 0.28**
W_1	**$S_sO\text{-}Eu^{2+}$**	1 S_wOH, 1 Eu^{3+}, −1 H^+	**1.80 ± 0.0**	**0.9 ± 0.0**
W_2	**$S_sO\text{-}EuCO_3$**	1 S_wOH, 1 Eu^{3+}, 1 HCO_3^-,-2 H^+,	**−1.10 ± 0.0**	**−2.48 ± 0.11**
W_3	**$S_sO\text{-}Eu(OH)_2$**	1 S_wOH, 1 Eu^{3+}, −3 H^+, 2H_2O	**−11.53 ± 0.32**	**−12.2 ± 0.29**
ThermoChimie				
Surface Species		**Composition**	**Na-IdP**	**Na-FBX**
			log K	**log K**
S_1	**$S_wO\text{-}Eu^{2+}$**	1 S_sOH, 1 Eu^{3+}, −1 H^+	**0.6 ± 0.0**	**−0.32 ± 0.16**
S_2	**$S_wO\text{-}EuCO_3$**	1 S_sOH, 1 Eu^{3+}, 1 CO_3^{2-}, −1 H^+	**6.60 ± 0.24**	**5.70 ± 0.0**
S_3	**$S_wO\text{-}Eu(OH)_2$**	1 S_sOH, 1 Eu^{3+}, −3 H^+, 2H_2O	**−18.38 ± 0.25**	**−17.16 ± 0.23**
W_1	**$S_sO\text{-}Eu^{2+}$**	1 S_wOH, 1 Eu^{3+}, −1 H^+	**2.25 ± 0.10**	**1.24 ± 0.24**
W_2	**$S_sO\text{-}EuCO_3$**	1 S_wOH, 1 Eu^{3+}, 1 CO_3^{2-}, −1 H^+	**8.43 ± 0.24**	**7.68 ± 0.18**
W_3	**$S_sO\text{-}Eu(OH)_2$**	1 S_wOH, 1 Eu^{3+}, −3 H^+, 2H_2O	**−16.38 ± 0.25**	**−16.02 ± 0.44**
Protonation/deprotonation reactions (From Missana et al., 2009a)				
Surface Species		**Composition**	**Na-FBX**	**Na-IdP**
			Log K	**Log K**
S_sO^-		1 S_sOH, −1 H^+	−9.9	−9.5
$S_sOH_2^+$		1 S_sOH, 1H^+	4.8	4.5
S_wO^-		1 S_wOH, −1 H^+	−8.4	−9.5
$S_wOH_2^+$		1 S_wOH, −1 H^+	5.3	5.9

physically unlikely (e.g. complexation of negatively charged species in negatively charged sites is discarded), or if additional spectroscopic or other evidence does not support them.

Table 1 summarises the reactions and mean values of the complexation constants used in this study to simulate the experimental data with both EQ (3)/6 and ThermoChimie databases. Further, Tables 5S (EQ (3)/6) and 6 S (ThermoChimie) list all the complexation constant details at each IS. The results of the simulations using EQ (3)/6 database are superimposed on the experimental data as continuous lines in Figs. 2–4. The simulations adequately reproduced the sorption behaviour under the experimental conditions for both clays. Fig. 5S in the Supporting Information shows the simulations based on the ThermoChimie database. As the use of either database satisfactory fit the experimental data, it is of great importance to note the need for accurate and up-to-date TDBs for critical contaminants.

As expected from the experimental data, the complexation constants of Na-IdP are higher than those of Na-FBX, with the exception of some cases given by Equation (8c). Note that the related SO-$Eu(OH)_2$ complex appears only at very high pH values, wherein sorption is almost quantitative, some precipitation is present, and the experimental error is the largest. For these reasons, determining its selectivity coefficient presents the highest uncertainty.

Another relevant point is related to the comparison between the main complexation constants obtained from each database. The constants related to Eu^{3+} complexation are very similar; in fact, Eu^{3+} has a similar behaviour in the speciation diagrams of both Figs. 1 and 2S. Conversely, the complexation constants related to $EuCO_3^+$ are approximately two orders of magnitude lower when the ThermoChimie TDB is used. This is logical, as the $EuCO_3^+$ concentration is predicted to have a much higher concentration in the ThermoChimie TBD than that in EQ (3)/6 database. The large differences observed for the complexation constants of $Eu(OH)_2^+$ are also expected because of their different formation constants, which result in different speciation diagrams.

Finally, regarding the simulated adsorption isotherms at neutral to basic pH values and a pH around 7, EQ (3)/6 TDB predicts the precipitation of solids, $Eu_2(CO_3)_3{:}3H_2O$ and $EuOHCO_3$, at Eu concentrations above 6×10^{-6} and 2×10^{-4} M, respectively. Meanwhile, the ThermoChimie TDB predicts the precipitation of $Eu(CO_3)(OH)(cr)$ at lower Eu concentrations, just above 2×10^{-8} M. The simulated isotherms at 2×10^{-1} M and a pH of 7.4 accounting for the contribution of these precipitated solids, is shown in Fig. 3b (dotted line). If a solid precipitates, the log (K_d) is expected to rapidly increase whereas, the experimental behaviour reveals a progressive decrease in the log (K_d). Nevertheless, even though the sorption isotherm simulations are quite good, at Eu equilibrium concentrations over 1×10^{-5} M and under neutral to alkaline pH values, they tend to systematically underestimate adsorption, and some Eu precipitation cannot be completely discarded above this concentration.

3.6. Sorption modelling: component additive approach

To model the sorption behaviour in the two Na-FBX and Na-IdP mixtures (50%/50% and 75%/25%) at an IS of 0.05 M, the constants determined for the individual components were used without any modifications. The model was superimposed on the experimental points as a continuous line (Fig. 5, EQ (3)/6, and Fig. 6S, ThermoChimie). The results show that the fit is quite good, indicating that Eu sorption in 2:1 clays is additive.

4. Conclusions

This study demonstrates that Eu adsorption onto mixtures of smectite and illite clays can be successfully predicted using a component additive model approach.

The Eu sorption behaviour observed in each of the studied clays was interpreted using the cation exchange and surface complexation. To evaluate the cation exchange and determine the selectivity coefficient for the Na–Eu exchange over an entire range of ISs, the competition between aluminium and divalent ions present in the solution were examined.

To interpret surface complexation, a 2-site non-electrostatic model was employed; a satisfactory data simulation was obtained

by considering the formation of monodentate surface complexes with Eu^{3+}, $EuCO_3^+$, and $Eu(OH)_2^+$ at both the strong and weak sites.

In the mixtures, higher quantities of smectite favoured Eu retention at pH values lower than 6, which is where cationic exchange predominates, because even though the selectivity coefficients for Na-IdP and Na-FBX are the same, ($log(^{Eu}_{Na}K_{SEL}) = 2.0$, the CEC of smectite is much higher than that of illite. At pH values greater than 6, in which surface complexation dominates, higher quantities of illite favour Eu retention because the complexation constants of illite are higher than those of smectite.

Simulations were performed considering two different TDBs that are available for europium. For both, satisfactory sorption fits in the single clay components as well as the mixed clays were obtained. The differences in the modelling results obtained using each TDB were highlighted, and the need for available and periodically updated thermodynamic data was emphasised. Any future update may require the revision of the selected complexation models.

This study evaluated Eu, as it is an element of interest in problems related to radioactive waste. However, mechanistic sorption modelling is applicable to broader environmental applications and can be conducted for other hazardous elements.

Credit author statement

Tiziana Missana, Funding acquisition, Conceptualization, Investigation, Formal analysis, Validation, Writing – original draft, Writing – review & editing. Ursula Alonso: Conceptualization, Investigation, Formal analysis, Validation, Writing – review & editing. Miguel Garcia: Conceptualization, Investigation, Formal analysis, Resources.

Declaration of competing interest

Authors declare no conflict of interest.

Acknowledgments

This study was partially supported by the FP6- EURATOM -NUWASTE (Grant ID: 516514) and by the Spanish Ministry of Science and Innovation (PID 2019-106398 GB-I00, ARNO Project).

Appendix A. Supplementary data

Supplementary data to this article can be found online at https://doi.org/10.1016/j.chemosphere.2021.129877.

References

Alessi, D.S., Fein, J.B., 2010. Cadmium adsorption to mixture soil components: testing the component additivity approach. Chem. Geol. 270 (1), 186–195.
Amman, L., Bergaya, F., Lagaly, G., 2005. Determination of the cation exchange capacity of clays with copper complexes revisited. Clay Miner. 40, 441–453.
Bergaya, F., Lagaly, G., 2013. Handbook of clay science. In: Development in Clay Science 5A. Elsevier.
Bonilla-Petriciolet, A., Mendoza-Castillo, D., Reynel-Avila, 2017. Adsorption Processes for Water Treatment and Purification. Springer.
Bradbury, M.H., Baeyens, B., 2005. Experimental and Modelling Investigations on Na-Illite: Acid Base Behaviour and the Sorption of Strontium, Nickel, Europium and Uranyl. PSI Bericht 05-02. Paul Sherrer Institute. PSI.
Bradbury, M.H., Baeyens, B., 2002. Sorption of Eu on Na and Ca montmorillonites: experimental investigation and modelling with cation exchange and surface complexation. Geochem. Cosmochim. Acta 66 (13), 2325–2334.
Bradbury, M.H., Baeyens, B., Geckeis, H., Rabung, T., 2005. Sorption of Eu(III)/Cm(III) on Ca-montmorillonite and Na-illite. Part 2: surface complexation modelling. Geochem. Cosmochim. Acta 69 (23), 5403–5412.
Bruggeman, C., Liu, D.J., Maes, N., 2010. Influence of Boom Clay organic matter on the adsorption of Eu by illite: geochemical modelling using the component additive approach. Radiochim. Acta 98, 597–605.
Cherif, M.A., Martin-Garin, A., Gerard, F., Bildstein, O., 2017. A robust and parsimonius model for cesium sorption on clay minerals and natural clay materials. Appl. Geochem. 87, 22–37.
Davis, J.A., Coston, J.A., Kent, D.B., Fuller, C.C., 1998. Application of the surface complexation concept to complex mineral assemblages. Environ. Sci. Technol. 32 (19), 2820–2828.
Delany, J.M., Lundeen, S.R., 1991. The LLNL Thermochemical Data Base – Revised Data and File Format for the EQ3/6 Package. Lawrence Livermore National Lab., CA (United States).
Dohrmann, R., Kaufhold, S., 2009. Three new, quick CEC methods for determining the amounts of exchangeable calcium cations in calcareous clays. Clay Clay Miner. 57, 338–352.
Fanghänel, Th, Neck, V., 2000. Comment on "Behaviour of europium(III) and its hydroxo and carbonate complexes in a solvent extraction system with HDBM in 2 M NaCl at 303 K" by M. Jimenez-Reyes, M. Solache-Rios, and A. Rojas-Hernandez. Radiochim. Acta 88, 499–501.
Fernandez, A.M., Baeyens, B., Bradbury, M.H., Rivas, P., 2004. Analysis of the pore water chemical composition of a Spanish compacted bentonite used in an engineered barrier. Phys. Chem. Earth 105–118.
Gabis, V., 1958. Etude preliminaire des argiles oligocenes du Puyen-Velay (Haute Loire). Bull. Soc. Franc. Mineral Cristallog. 183–185.
Gaines, G.I., Thomas, H.C., 1953. Adsorption studies on clay minerals. II. A formulation of the thermodynamics of exchange adsorption. J. Chem. Phys. 21, 714–718.
Goldberg, S., 2014. Modeling selenate adsorption behaviour on oxides, clay minerals and soils using the triple layer model. Soil Sci. 179, 568–576.
Grivé, M., Duro, L., Colás, E., Giffaut, E., 2014. Thermodynamic data selection applied to radionuclides and chemotoxic elements: an overview of the TermoChimie TDB. Appl. Geochem. 55, 85–94.
Guillamont, R., Fanghanel, T., Neck, V., Fuger, J., Palmer, D.A., Grenthe, I., Rand, M.H., 2003. Update on the chemical thermodynamics of uranium, neptunium, plutonium, americium and technetium. In: Mompean, F.J.I.M. (Ed.), Issy-les-Moulineaux, France. OECD Nuclear Energy Agency, Data Bank.
Guo, Z., Xu, J., Shi, K., Tang, Y., Wu, W., Tao, Z., 2009. Eu(III) adsorption/desorption studies on Na-bentonite: experimental and modelling studies. Colloids Surf., A 339, 126–133.
Huertas, F., Fariña, P., Farias, J., García-Siñeriz, J.L., Villar, A.M., Fernández, A.M., Martín, P.L., Elorza, F.J., Gens, A., Sánchez, M., Lloret, A., Samper, J., Martínez, M.A., 2006. FEBEX Project. Full-Scale Engineered Barriers Experiment for a Deep Geological Repository for High Level Radioactive Waste in Crystalline Host Rock. Updated Final Report 1994-2004. ENRESA, Madrid.
Huittinen, N., Rabung, Th, Andrieux, P., Letho, J., Geckeis, H., 2010. A comparative batch sorption and time-resolved laser fluorescence spectroscopy study on the sorption of Eu(III) and Cm(III) on synthetic and natural kaolinite. Radiochim. Acta 98, 613–620.
Hurel, C., Marmier, M., 2010. Sorption of europium on a MX-80 bentonite sample: experimental and modelling results. J. Radioanal. Nucl. Chem. 284, 225–230.
Kowal-Fouchard, A., Drot, R., Simoni, E., Erhardt, J.J., 2004b. Use of spectroscopic techniques for U(VI)/montmorillonite interaction modelling. Environ. Sci. Technol. 38, 1399–1407.
Kowal-Fouchard, Drot, R., Simoni, E., Marmier, N., Fromage, F., Erhardt, J., 2004a. Structural identification of Eu(III) adsorption complexes on montmorillonite. New J. Chem. 28, 864–869.
Kumar, S., Pente, A.S., Bajpai, R.K., Kaushik, C.P., Tomar, B.S., 2013. Americium sorption on smectite-rich natural clay from granitic groundwater. Appl. Geochem. 35, 28–34.
Landry, C.J., Koretsky, C.M., Lund, T.J., Schaller, M., Das, S., 2009. Surface complexation modeling of Co(II) adsorption on mixtures of hydrous ferric oxide, quartz and kaolinite. Geochem. Cosmochim. Acta 73 (13), 3723–3737.
Marques Fernandes, M., Baeyens, B., Bradbury, M.H., 2008. The influence of carbonate complexation on lanthanide/actinide sorption on montmorillonite. Radiochim. Acta 96, 691–697.
Marques Fernandes, M., Scheinost, A.C., Baeyens, B., 2016. Sorption of trivalent lanthanides and actinides onto montmorillonite: macroscopic, thermodynamic and structural evidence for ternary hydroxo and carbonate surface complexes on multiple sorption sites. Water Res. 99, 74–82.
Mayordomo, N., Alonso, U., Missana, T., 2016. Analysis of the improvement of selenite retention in smectite by adding alumina nanoparticles. Sci. Total Environ. 572, 1025–1032.
Mayordomo, N., Alonso, U., Missana, T., 2019. Effects of γ-alumina nanoparticles on strontium sorption in smectite: additive model approach. Appl. Geochem. 100, 121–130.
Missana, T., Alonso, U., Fernández, A.M., García-Gutiérrez, M., 2018a. Analysis of the stability beaviour of colloids obtained from different smectite clays. Appl. Geochem. 92, 180–187.
Missana, T., Alonso, U., Fernández, A.M., García-Gutiérrez, M., 2018b. Colloidal properties of different smectite clays: significance for the bentonite barrier erosion and radionuclide transport in radioactive waste repositories. Appl. Geochem. 97, 157–166.
Missana, T., Alonso, U., García-Gutiérrez, M., 2009a. Experimental study and modelling of selenite sorption onto illite and smectite clays. J. Colloid Interface Sci. 334, 132–138.
Missana, T., Alonso, U., García-Gutiérrez, M., Albarran, N., López, T., 2009b. Experimental and modelling study of U(VI) sorption onto a Spanish smectite. Mater. Res. Soc. Symp. Proc. 1124, 1–5 (1124-Q07-05).

Missana, T., Alonso, U., García-Gutiérrez, M., Mingarro, M., 2008. Role of bentonite colloids on europium and plutonium migration in a granite fracture. Appl. Geochem. 23, 1484–1497.
Missana, T., Benedicto, A., García-Gutiérrez, M., Alonso, U., 2014. Modeling cesium retention onto Na-, Ca- and K-smectite: effects of ionic strenght, exchange and competing ions on the determination of selectivity coefficients. Geochem. Cosmochim. Acta 128, 266–277.
Norris, S., 2014. Clays in Natural and Engineered Barriers for Radioactive Waste Confinement: an Introduction. Geological Society London Special Publications, London.
Odom, I., 1984. Smectite clay minerals: properties and uses. Phylosophical transactions of the royal society of london. Series A, Mathematical and physical Sciences 311, 391–409.
Payne, T.E., Brendler, V., Ochs, M., Baeyens, B., Brown, P.L., Davis, J.A., Eckberg, C., Kulik, D.A., Lutzenkirchen, J., Missana, T., Tachi, Y., Van Loon, L.R., Altmann, S., 2013. Guidelines for thermodynamic sorption modelling in the context of radioactive waste disposal. Environ. Model. Software 42, 143–156.
Plancque, G., Moulin, V., Toulhoat, P., Moulin, C., 2003. Europium speciation by time-resolved laser-induced fluorescence. Anal. Chim. Acta 478, 11–22.
Rabung, T., Pierret, M.C., Bauer, A., Geckeis, H., Bradbury, M.H., Baeyens, B., 2005. Sorption of Eu(III)/Cm(III) on Ca-montmorillonite and Na-illite. Part I: batch sorption and time-resolved laser fluorescence spectroscopy experiments. Geochem. Cosmochim. Acta 69, 5393–5402.
Rao, R.R., Chatt, A., 1988. Characterization of Eu(III) carbonate complexes in simulated groundwater by solven extraction. J. Radioanal. Nucl. Chem. 124 (1), 211–225.
Runde, W., Meinrath, G., Kim, J., 1992. A study of solid-liquid phase equilibria of trivalent lanthanide and actinide ions in carbonate systems. Radiochim. Acta 58/59, 93–100.
Sasaki, T., Ueda, K., Saito, T., Aoyagi, N., Kobayashi, I., Takagi, I., Kimura, T., Tachi, Y., 2016. Sorption of Eu3+ on Na-montmorillonite studied by time-resolved laser fluorescence spectroscopy and surface complexation modelling. J. Nucl. Sci. Technol. 53, 592–601.
Schnurr, A., Marsac, R., Rabung, T., Lutzenkirchen, J., Geckeis, H., 2015. Sorption of Cm(III) and Eu(III) onto clay minerals under saline conditions: batch adsorption, laser fluorescence spectroscopy and modelling. Geochem. Cosmochim. Acta 151, 192–202.
Sellin, P., Leupin, X.O., 2014. The use of clay as an engineered barrier in radioactive waste management. A review. Clay and Clay Minerals 1 (6), 477–498.
Sheng, G.D., Shao, D.D., Fan, Q.H., Xu, D., Chen, Y.X., Wang, X.K., 2009. Effect of pH and ionic strenght of sorption of Eu(III) to MX-80 bentonite: batch and XAFS study. Radiochim. Acta 97, 621–630.
Spahiu, K., Bruno, J., 1995. A Selected Thermodynamic Database for REE to Be Used in HLNW Performance Assessment Exercises SKB. SKB Technical Report TR95-35, Sweden.
Stumpf, T., Henning, C., Bauer, A., Denecke, M.A., Fanghänel, T., 2004. An EXAFS and TRLFS study of the sorption of trivalent actinides onto smectite and kaolinite. Radiochim. Acta 92, 133–138.
Tertre, E., Berger, G., Castet, S., Loubet, M., Giffaut, E., 2005. Experimental sorption of Ni2+, Cs+ and Ln3+ onto a montmorillonite up to 150 °C. Geochem. Cosmochim. Acta 69 (21), 4937–4948.
Tertre, E., Berger, G., Simoni, E., Castet, S., Giffaut, E., Loubet, M., Catalette, H., 2006. Europium retention onto clay minerals from 25 to 150 °C: experimental measurements, spectroscopic features and sorption modleiing. Geochem. Cosmochim. Acta 70, 4563–4578.
Van der Lee, J., de Windt, L., 1999. CHESS Tutorial and Cookbook Technical Report LHM/RD/99/05.
Vercouter, T., Vitorge, P., Trigoulet, N., Giffaut, E., Moulin, C., 2005. Eu(CO3)33- and the limiting carbonate complexes of other M3+ f-elements in aqueous solutions: a solubility and TRLFS study. New J. Chem. 29 (4), 544–553.
Verma, P.K., Semenkova, A.S., Krupskaya, V.V., Zakusin, S.V., Mohapatra, P.K., Romanchuk, A.Y., Kalmykov, S.N., 2019. Eu(III) sorption onto various montmorillonite: experiments and modelling. Appl. Clay Sci. 175, 22–29.